

Design and Realization of a Linear Magnetic Gear

Robert C. Holehouse, Kais Atallah, and Jiabin Wang

Department of Electronic and Electrical Engineering, The University of Sheffield, Sheffield S1 3JD, U.K.

This paper describes a 3.25:1 linear magnetic gear which has been designed and prototyped to meet the performance requirements of an aerospace application. It has been shown that the force capability of the linear magnetic gear is very sensitive to the spacing between the pole-piece rings and that a 5% reduction in the distance between pole pieces may result in a 30% decrease in force transmission capability. It has also been shown that for a given output stroke requirement, in order to maximize volumetric force density, magnetic designs with large airgap diameters and shorter high-speed armature axial lengths would be preferred.

Index Terms—Linear machine, linear magnetic gear, permanent magnets.

I. INTRODUCTION

THE increasing demand for high force density linear actuators is currently being met almost exclusively by employing a hydraulic actuator or an electromechanical actuator with a lead/ball/rollerscrew and nut to transform rotary motion to linear motion. However, in addition to the poor hydraulic power transmission density, the reliability and maintenance requirements of both actuation systems as well the higher risk of jamming of electromechanical actuators can be significant issues.

Therefore, despite their relatively poor thrust force density, linear electromagnetic actuators are increasingly being considered for applications spanning from industrial automation to automotive active suspension [1], [2]. An alternative approach to increase the force transmission capability of electromagnetic actuators is to employ a linear magnetic gear with a linear brushless permanent-magnet machine [3], [4].

Further, since a linear magnetic gear exhibits inherent overload protection, viz. when the output armature is subjected to a load force which is larger than the pull-out force, it will slip harmlessly, thereby preventing physical damage to the magnetic gear and the systems connected to it. This feature is very important for aerospace applications.

The paper describes a 3.25:1 linear magnetic gear which has been designed and prototyped to meet the performance requirements of an aerospace application. It has been shown that manufacturing tolerances can have a significant effect on transmitted force capability.

II. FORCE DENSITY

The linear magnetic gear considered in this paper has the same principle of operation as the rotary magnetic gear described in [5]–[8]. It consists of three tubular armatures with the outer and inner carrying arrays of permanent magnets having different numbers of poles and the intermediate having a set of

annular ferromagnetic pole pieces (Fig. 1), which modulate the magnetic fields produced by the magnet arrays.

It may be shown [3] that when the outer permanent-magnet armature is kept stationary, the gear ratio between high-speed armature (inner permanent magnet armature) and pole-piece armature is given by

$$G_r = \frac{n_s}{p} \quad (1)$$

where n_s is the number of active ferromagnetic pole pieces and p is the number of pole pairs on the high-speed armature.

In [3], it was shown that an active force density of 2 MN/m³ could be achieved. However, unlike rotary magnetic gears, not all magnetic components are simultaneously contributing to force transmission, therefore, the magnetic volumetric force density, where the volume V_G encompassing all of the magnetic components is considered, depends on the stroke and gear ratio.

If δ_A is the active force density, where only the volume V_A of the magnetic components active at any instant of time is considered, the transmitted force is given by

$$F = \delta_A V_A. \quad (2)$$

For a gear ratio G_r , an output stroke S and a high-speed armature of active length L_A , the total length of the gear will be

$$L_G = L_A + G_r S \quad (3)$$

and

$$V_G = \frac{V_A}{L_A} (L_A + G_r S) = \frac{F}{\delta_A} \left(1 + G_r \frac{S}{L_A} \right) \quad (4)$$

resulting in a volumetric force density

$$\delta_G = \frac{\delta_A}{1 + G_r \frac{S}{L_A}}. \quad (5)$$

Fig. 2 shows the variation of the gear force density with the gear ratio. It can be seen that the highest force density is achieved when the output stroke is significantly shorter than the length of the high-speed armature. It can also be seen that the force density decreases with an increasing gear ratio.

For many applications, with a specified output stroke and force requirement, it is the overall system force density that is of most interest (i.e., the combined density of the gear and the high-speed low-force machine driving it). If a machine of force

Manuscript received February 21, 2011; accepted May 07, 2011. Date of current version September 23, 2011. Corresponding author: K. Atallah (e-mail: k.atallah@sheffield.ac.uk).

Color versions of one or more of the figures in this paper are available online at <http://ieeexplore.ieee.org>.

Digital Object Identifier 10.1109/TMAG.2011.2157101

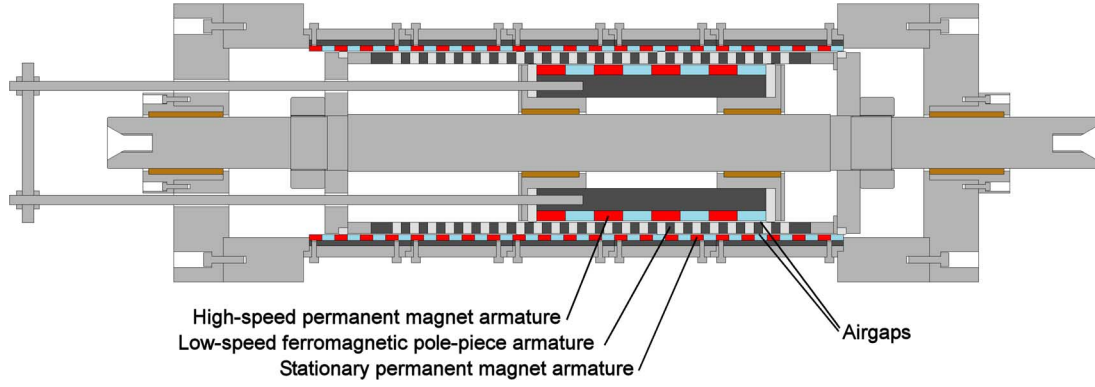


Fig. 1. Cross-sectional schematic of the prototype linear magnetic gear.

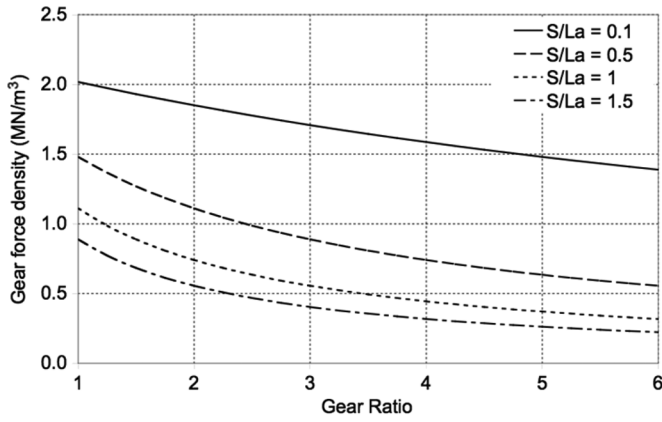


Fig. 2. Variation of gear force density with gear ratio.

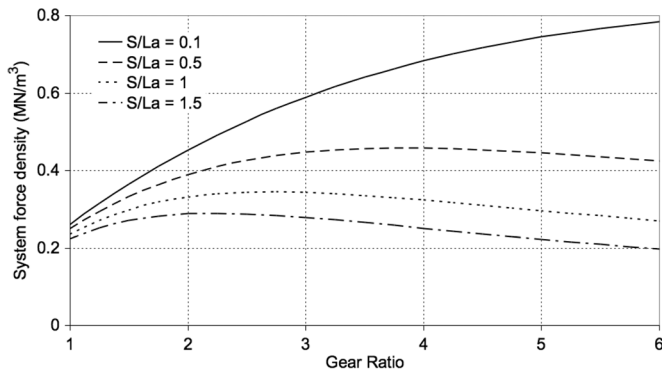


Fig. 3. Variation of system force density with the gear ratio.

TABLE I
LEADING DIMENSIONS OF THE MAGNETIC GEAR

Number of pole-pairs on high-speed armature	4
Number of active pole-pairs on stationary armature	9
Number of active ferromagnetic pole-pieces	13
Active length of high-speed armature	200mm
Active stator diameter	180mm
Airgap diameter	160mm
Airgap length	1mm
Radial pole-piece thickness	10mm
Magnet material NdFeB	$B_r = 1.2T$

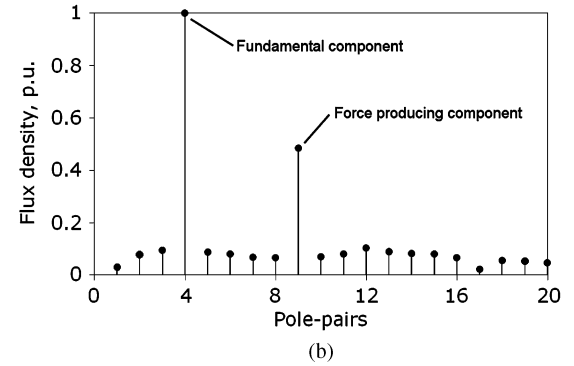
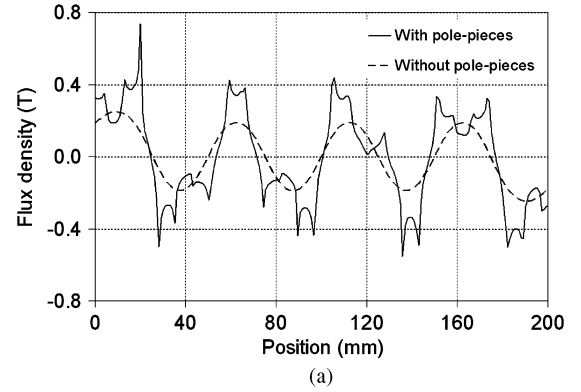


Fig. 4. Radial flux density in the airgap adjacent to the stationary armature due to high-speed armature magnets. (a) Flux density waveform. (b) Harmonic spectrum with pole pieces.

density δ_{mach} is employed to drive the magnetic gear, its volume will be given by

$$V_{mach} = \frac{F}{G_r} \frac{1}{\delta_{mach}} \quad (6)$$

resulting in a total volume

$$V_{system} = F \left(\frac{1}{G_r} \frac{1}{\delta_{mach}} + \frac{1}{\delta_A} + G_r \frac{1}{\delta_A} \frac{S}{L_A} \right) \quad (7)$$

and a force density

$$\delta_{system} = \frac{\delta_A}{1 + \frac{1}{G_r} \frac{\delta_A}{\delta_{mach}} + G_r \frac{S}{L_A}} \quad (8)$$

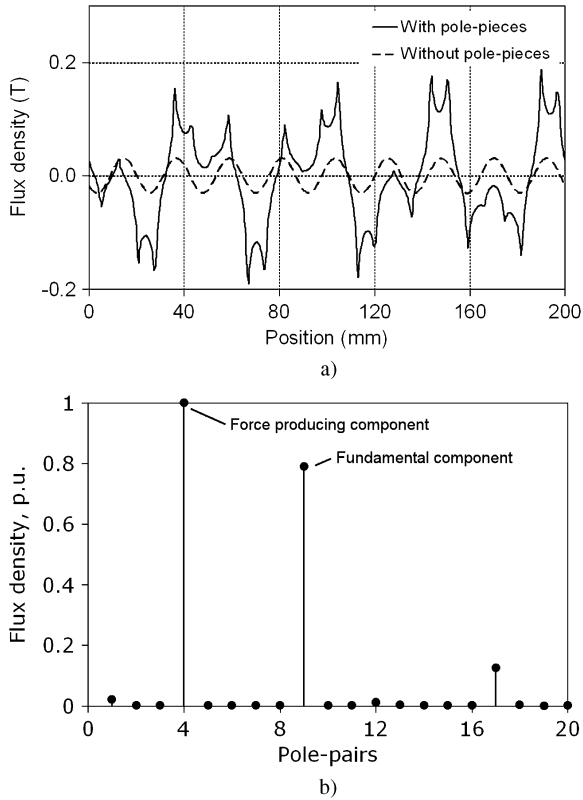


Fig. 5. Radial flux density in the airgap adjacent to the high-speed armature due to stationary armature magnets. (a) Flux density waveform. (b) Harmonic spectrum with pole pieces.

Fig. 3 shows the force density of a system comprising a linear magnetic gear coupled to a naturally cooled PM linear machine (force density 300 kN/m^3). It can be seen that the system force density is again highest when the required output stroke is significantly shorter than the active length of the high-speed armature. It can also be seen that for any ratio of output stroke to active length, a gear ratio exists for which an optimum system density exists.

III. SIMULATION STUDIES

Finite-element analysis has been employed for the design and analysis of the gear, whose leading dimensions are given in Table I.

Figs. 4 and 5 show the radial flux density in the airgaps adjacent to the high-speed and stationary armatures, respectively, and their associated space harmonic spectra. It can be seen that the introduction of the ferromagnetic pole pieces results in an asynchronous harmonic having the same number of poles as the permanent magnets of the other armature.

When the diameter of the airgap adjacent to the stationary armature and the volume of the permanent magnets are fixed, Fig. 6 shows the effect of the radial thickness of the pole pieces on the transmitted force. It is seen there that an optimum thickness exists for which the transmitted force is maximum.

IV. DEMONSTRATOR MAGNETIC GEAR

The linear magnetic gear, whose leading dimensions are given in Table I, has been constructed. A cross-sectional

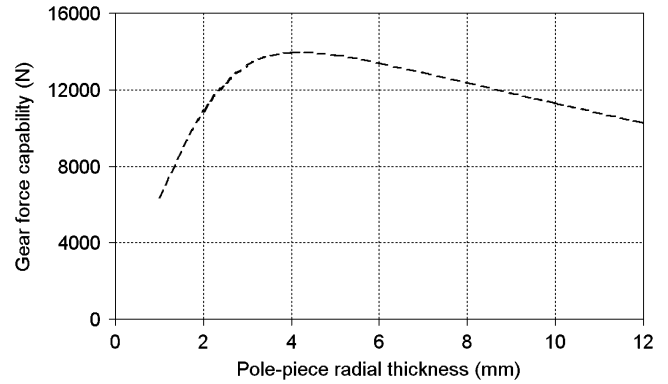


Fig. 6. Variation in force capability with pole-piece radial thickness.

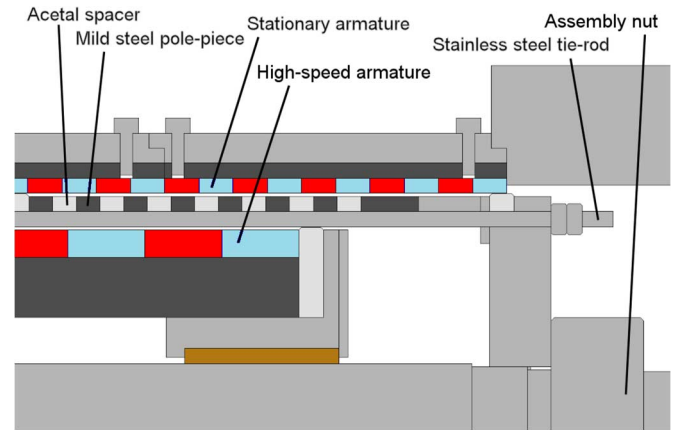


Fig. 7. Schematic of magnetic gear (a close-up view).

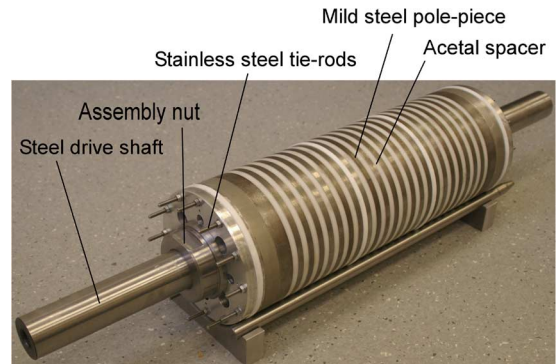


Fig. 8. Pole-piece armature with an integrated high-speed armature.

schematic is shown in Fig. 1, and a more enlarged section is shown in Fig. 7. Fig. 8 shows the assembled pole-piece armature while Fig. 9 shows the linear magnetic gear on the test bed.

Fig. 10 compares the measured and predicted variations of the transmitted force on the pole-piece armature with the position when the high-speed armature is kept stationary. It can be seen that the measured force is markedly lower than was predicted. This may be attributed to the mechanical construction of the pole-piece armature, where spacing between the pole-piece rings is maintained by polymer spacer rings (Figs. 7 and 8), whose axial dimensions could have exhibited large reductions



Fig. 9. Magnetic gear on the test bed.

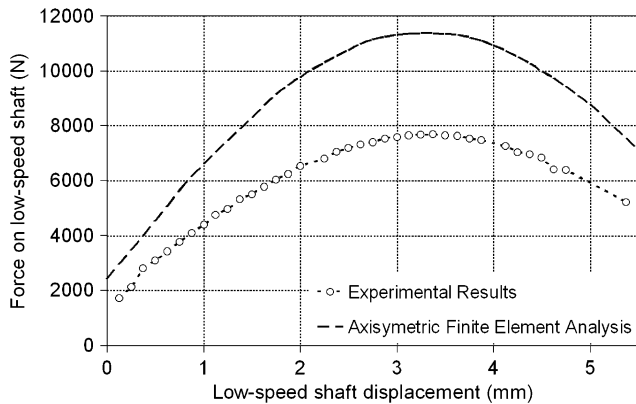


Fig. 10. Variation of measured and predicted force on the pole-piece armature with position. (Locked high-speed armature).

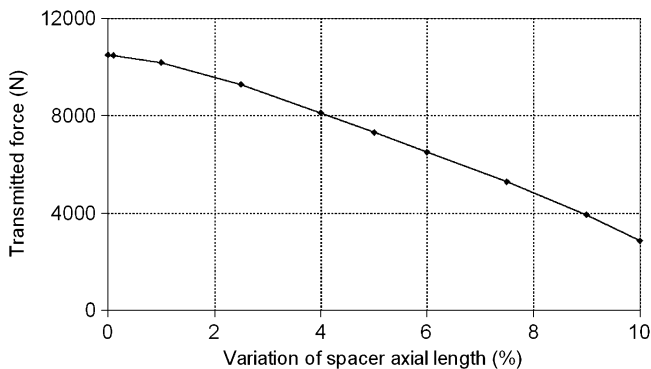


Fig. 11. Variation of transmitted force with the change of axial distance between the pole-piece rings.

when subjected to large and repeated compressive stresses applied by the tie-rods and the assembly nut. In order to illustrate the sensitivity of the transmitted force to manufacturing tolerances, Fig. 11 shows the variation of the transmitted force with

the relative change of the dimensions of the spacers from the design value. It can be seen that a 5% reduction in the axial dimension of the spacers results in a 30% reduction in the transmitted force capability.

It may be worth noting that the spacers employed in this gear have a very low compressive modulus; therefore, a 5% reduction in axial dimensions is highly probable due to the high levels of force employed to compress the pole-piece armature in order to ensure mechanical stiffness.

V. CONCLUSION

A linear magnetic gear has been presented, and predicted and measured transmitted forces have been compared. It has been shown that the spacing between the pole-piece rings has a significant effect on the transmitted force, in that a 5% reduction in the axial dimensions of spacers can result in a 30% reduction in the force transmission. It has also been shown that a high force density of a system comprising a linear machine and magnetic gear can be achieved.

ACKNOWLEDGMENT

The authors would like to acknowledge the support of the U.K. Engineering and Physical Science Research Council, EPSRC, for the award of a studentship. The authors would like to thank J. Wilkinson for his support and assistance in the design and construction of the prototype gear and associated test rig.

REFERENCES

- [1] J. Wang, W. Wang, K. Atallah, and D. Howe, "Demagnetisation assessment for three-phase tubular permanent magnet brushless machines," *IEEE Trans. Magn.*, vol. 44, no. 9, pp. 2195–2203, Sep. 2008.
- [2] J. Wang, K. Atallah, and D. Howe, "Design considerations of tubular flux-switching permanent magnet machines," *IEEE Trans. Magn.*, vol. 44, no. 11, pp. 4026–4032, Nov. 2008.
- [3] K. Atallah, J. Wang, S. Mezani, and D. Howe, "A novel high-performance linear magnetic gear," *Inst. Elect. Eng. J. Trans. Ind. Appl.*, vol. 126, no. 10, 2006.
- [4] W. Li, K. T. Chau, and J. Li, "Simulation of a tubular linear magnetic gear using hts bulks for field modulation," *IEEE Trans. Appl. Supercond.*, vol. 21, no. 3, pp. 1167–1170, Jun. 2011.
- [5] K. Atallah and D. Howe, "A novel high-performance magnetic gear," *IEEE Trans. Magn.*, vol. 37, no. 4, pp. 2844–2866, Jul. 2001.
- [6] K. Atallah, S. Claverley, and D. Howe, "Design, analysis and realisation of a high-performance magnetic gear," *Proc. IEEE. Power Appl.*, vol. 151, no. 2, pp. 135–143, Mar. 2004.
- [7] P. Rasmussen, T. Andersen, F. Jorgensen, and O. Nielsen, "Development of a high-performance magnetic gear," *IEEE Trans. Ind. Appl.*, vol. 41, no. 3, pp. 764–770, May/Jun. 2005.
- [8] E. Gouda, S. Mezani, L. Baghli, and A. Rezzoug, "Comparative study between mechanical and magnetic planetary gears," *IEEE Trans. Magn.*, vol. 47, no. 2, pp. 439–450, Feb. 2011.